Inorg. Chem. **2007**, *46*, 6902–6910

Structure and Properties of Dinuclear Manganese(III) Complexes with Pentaanionic Pentadentate Ligands Including Alkoxo, Amido, and Phenoxo Donors

Liliana Stoicescu,[†,‡] Aurélie Jeanson,[†] Carine Duhayon,[†] Ana Tesouro-Vallina,[†] Athanassios K. Boudalis,[§] Jean-Pierre Costes,[†] and Jean-Pierre Tuchagues*[,†]

Laboratoire de Chimie de Coordination du CNRS, UPR 8241, 205 route de Narbonne, 31077 Toulouse Cedex 04, France, and Institute of Materials Science, NCSR "Demokritos", 153 10 Aghia Paraskevi Attikis, Greece

Received December 15, 2006

Doubly bridged μ-alkoxo-μ-X (X = pyrazolato or acetato) dinuclear Mn^{III} complexes of 2-hydroxy-*N*-{2-hydroxy-3-[(2-hydroxybenzoyl)amino]propyl}benzamide) (H_5L^1) and 2-hydroxy-*N*-{2-hydroxy-4-[(2-hydroxybenzoyl)amino]-butyl}benzamide (H_5L^2), $[Mn_2(L)(pz)(MeOH)_4]\cdot x$MeOH (**1**, L = L^1, $x = 0.5$; **2**, L = L^2, $x = 0$; Hpz = pyrazole) and $[Mn_2(L^1)(OAc)(MeOH)_4]$ (**3**), have been prepared, and their structure and magnetic properties have been studied. The X-ray diffraction analysis of **1** ($C_{24.5}H_{34}Mn_2N_4O_{9.5}$, triclinic, $P\bar{1}$, $a = 12.2050(7)$ Å, $b = 12.7360(8)$ Å, $c = 19.2780(10)$ Å, $\alpha = 99.735(5)°$, $\beta = 96.003(4)°$, $\gamma = 101.221(5)°$, $V = 2867.6(3)$ Å^3, $Z = 4$), **2** ($C_{25}H_{34}Mn_2N_4O_9$, triclinic, $P\bar{1}$, $a = 9.4560(5)$ Å, $b = 11.0112(5)$ Å, $c = 13.8831(6)$ Å, $\alpha = 90.821(4)°$, $\beta = 92.597(4)°$, $\gamma = 93.403(4)°$, $V = 1441.29(12)$ Å^3, $Z = 2$), and **3** ($C_{23}H_{32}Mn_2N_2O_{11}$, triclinic, $P\bar{1}$, $a = 10.511(5)$ Å, $b = 11.713(5)$ Å, $c = 13.135(5)$ Å, $\alpha = 64.401(5)°$, $\beta = 74.000(5)°$, $\gamma = 66.774(5)°$, $V = 1329.3(10)$ Å^3, $Z = 2$) revealed that all complexes consist of dinuclear units which are further extended into 1D (**1** and **3**) and 2D (**2**) supramolecular networks via hydrogen-bonding interactions. Magnetic susceptibility data evidence antiferromagnetic interactions for all three complexes: $J = -3.6$ cm^{-1}, $D \approx 0$ cm^{-1}, $g = 1.93$ (**1**); $J = -2.7$ cm^{-1}, $D = 0.8$ cm^{-1}, $g = 1.93$ (**2**); $J = -4.9$ cm^{-1}, $D = 3.8$ cm^{-1}, $g = 1.95$ (**3**).

Introduction

In the past decades, considerable attention has been dedicated to the synthesis of hetero-bridged μ-alkoxo-μ-X and μ-alkoxo-μ-X-μ-Y (X, Y = carboxylato, pyrazolato, azido, cyanato, nitrito, hydroxo, methoxo) dinuclear transition metal complexes.[1−8] This ensues from their various interesting biomimetic and magnetic properties. The pentadentate dinucleating Schiff base ligands and the *N*,*N*,*N*′,*N*′-tetrasubstituted-1,*n*-diamino-*n*′-hydroxyalkanes (*n*, *n*′ = 3, 2; 4, 2, and 5, 3) having an endogenous alkoxo bridge have been used extensively to obtain doubly or triply bridged dinuclear complexes of copper,[1] manganese,[2] iron,[3] nickel,[4] cobalt,[5] vanadium,[6] and zinc.[7] So far, very few structurally characterized doubly bridged μ-alkoxo-μ-acetato[2d] and μ-alkoxo-μ-pyrazolato[2c] manganese(II) and μ-alkoxo-μ-methoxo manganese(III)[2a,b] dinuclear complexes based on these types of ligands have been reported. The structurally characterized Mn^{II} complex $[Mn_2(L)(OAc)(butanol)](ClO_4)_2\cdot H_2O$[2d] includes a μ-alkoxo bridge from the ligand HL (*N*,*N*,*N*′,*N*′-tetrakis(2-methylenebenzamidazolyl)-1,3-diaminopropan-2-ol). However, there are no structural informations on μ-alkoxo-μ-pyrazolato dinuclear manganese complexes. The unique report concerning a manganese(II) complex of this type[2c] was based only on analytical and spectroscopic data. From a dinucleating ligand incorporating (2-hydroxybenzamide) moieties, Bertoncello et al.[8] have obtained doubly bridged (μ-alkoxo)(μ-acetato)dimanganese(III) complexes of general formula $[Mn_2(L^1)(OAc)(B_4)]$, where B = pyridine, γ-picoline, and methanol. Only the molecular structure of the pyridine derivative $[Mn_2(L^1)(OAc)(py)_4]\cdot py\cdot H_2O$ (H_5L^1 = 2-hydroxy-*N*-{2-hydroxy-3-[(2-hydroxybenzoyl)amino]-

* To whom correspondence should be addressed. E-mail: jean-pierre.tuchagues@lcc-toulouse.fr. Fax: (+33)561533003.
† Laboratoire de Chimie de Coordination du CNRS.
‡ On leave from the University of Bucharest, Faculty of Chemistry, Inorganic Chemistry Department, 23 Dumbrava Roşie, 020464 Bucharest, Romania.
§ Institute of Materials Science.

10.1021/ic062398r CCC: $37.00
Published on Web 07/25/2007

propyl}benzamide) was described revealing that this complex exists as discrete molecules.

In this study, we describe the synthesis, crystal structure, and magnetic properties of three doubly bridged μ-alkoxo-μ-X (X = pyrazolato or acetato) dinuclear manganese(III) complexes: $[Mn_2(L)(pz)(MeOH)_4]\cdot x$MeOH (**1**, L = L^1, x = 0.5; **2**, L = L^2, x = 0; H_5L^2 = 2-hydroxy-*N*-{2-hydroxy-4-[(2-hydroxybenzoyl)amino]butyl}benzamide; Hpz = pyrazole) and $[Mn_2(L^1)(OAc)(MeOH)_4]$ (**3**).

Experimental Section

Materials. All reagents and solvents used in this study are commercially available (Aldrich or Fluka) and were used without further purification. All syntheses were carried out in aerobic conditions.

Caution! The perchlorate salts of metal complexes with organic ligands are potentially explosive. Only small quantities of compounds should be prepared, and they should be handled with much care!

Ligands. H_5L^1. A mixture of phenyl salicylate (2.142 g, 10 mmol), Et_3N (1.38 mL, 10 mmol), and 1,3-diaminopropan-2-ol (0.45 g, 5 mmol) in propan-2-ol (20 mL) was heated at about 60 °C for 5 h under stirring. The solution was concentrated at about 5 mL, and the white precipitate which appeared upon cooling was filtered off, washed with CH_2Cl_2, and dried. Yield: 1.18 g (71.4%). Anal. Calcd for $C_{17}H_{18}N_2O_5$: C, 61.81; H, 5.49; N, 8.49. Found: C, 61.7; H, 5.1; N, 8.2. IR (KBr pellet, cm^{-1}): 3377, 3083 (ν_{OH} and ν_{NH}), 1640 ($\nu_{C=O}$), 1253 (ν_{CO}(phenoxo)), 1055 (ν_{CO}(alkoxo)). UV−vis (λ_{max}, nm): 370. ^{1}H NMR (250 MHz, 20 °C, DMSO-d_6) (δ, ppm): 3.46−3.48 (m, 4H, CH_2), 3.98 (m, 1H, C*H*), 5.87 (s, 1H, CHO*H*), 6.99 (d, J = 7.8 Hz, 2H, ArC(3)*H*), 7.02 (t, 8.0 Hz, 2H, ArC(5)*H*), 7.5 (t, J = 7.8 Hz, 2H, ArC(4)*H*), 8.00 (d, J = 8.0 Hz, ArC(6)*H*), 9.07 (b, 2H, N*H*), 12.54 (s, 2H, ArC(2)O*H*). ^{13}C NMR (δ, ppm): 43.38 (*C*H2), 67.99 (*C*HOH), 115.95 (Ar*C*(3)H), 117.49 (Ar*C*(1)), 118.55 (Ar*C*(5)H), 128.41 (Ar*C*(6)H), 133.64 (Ar*C*(4)H), 159.94 (Ar*C*(2)OH), 168.7 (O*C*NH).

H_5L^2. 1,4-Diaminobutan-2-ol dihydrochloride was synthesized according to a reported method.[9] 1,4-Diaminobutan-2-ol was obtained by reaction of its hydrochloride salt (0.708 g, 4 mmol) with potassium *tert*-butoxide (0.897 g, 8 mmol) in ethanol (25 mL). The KCl precipitate was filtered off, and the filtrate was mixed with a solution of phenyl salicylate (3.426 g, 16 mmol) and Et_3N (2.22 mL, 16 mmol) in propan-2-ol (30 mL). The reaction mixture was stirred at room temperature for 2 h and then warmed at about 60 °C for 12 h. The obtained solution was left to stand overnight at room temperature. Addition of CH_2Cl_2 yielded a white precipitate that was filtered off, washed with CH_2Cl_2, and dried. Yield: 0.42 g (30.5%). Anal. Calcd for $C_{18}H_{20}N_2O_5$: C, 62.78; H, 5.85; N, 8.13. Found: C, 62.3; H, 5.6; N, 7.9. IR (KBr pellet, cm^{-1}): 3495, 3396, 3057 (ν_{OH} and ν_{NH}), 1640 ($\nu_{C=O}$), 1253, 1243 (ν_{CO}(phenoxo)), 1076 (ν_{CO}(alkoxo)). UV−vis (λ_{max}, nm): 354. ^{1}H NMR (250 MHz, 20 °C, DMSO-d_6) (δ, ppm): 1.71 (m, 2H, CHCH_2CH$_2$), 3.35−3.61 (m, 4H, CH_2CH and CHCH$_2$CH_2), 3.85 (b, 1H, C*H*), 5.14 (s, 1H, CHO*H*), 6.95−7.02 (m, 4H, ArC(3)*H*, ArC(3′)*H*, ArC(5)*H*, ArC(5′)*H*), 7.48−7.52 (m, 2H, ArC(4)*H*, ArC(4′)*H*), 7.95−8.01 (m, 2H, ArC(6)*H*, ArC(6′)*H*), 8.96 (t, J = 5.3 Hz, 2H, N*H*), 12.69 (s, 2H, ArC(2)O*H*). ^{13}C-NMR (δ, ppm): 34.28 (CH*C*H$_2$CH$_2$), 36.35 (CHCH$_2$*C*H$_2$), 45.51 (CH$_2$*C*H), 67.03 (*C*H), 115.33 and 115.79 (Ar*C*(3)H and Ar*C*(3′)H), 117.42 and 117.51 (Ar*C*(1) and Ar*C*(1′)), 118.61 and 118.67 (Ar*C*(5)H and Ar*C*(5′)H), 127.75 and 128.32 (Ar*C*(6)H and Ar*C*(6′)H), 133.67 and 133.73 (Ar*C*(4)H and Ar*C*(4′)H), 159.84 and 160.27 (Ar*C*(2)H and Ar*C*(2′)H), 168.76 and 169.06 (O*C*NH).

Complexes. $[Mn_2(L^1)(pz)(MeOH)_4]\cdot 0.5$MeOH (1). To a stirred solution of H_5L^1 (0.033 g, 0.1 mmol) in MeOH (10 mL) was added a solution of $Mn(ClO_4)_2\cdot 6H_2O$ (0.072 g, 0.2 mmol) in 10 mL of MeOH, piperidine (0.049 mL, 0.5 mmol), and a solution of pyrazole (0.014 g, 0.2 mmol) in 10 mL of MeOH. The reaction mixture

(1) (a) Nakao, Y.; Takagi, Y.; Okazaki, H.; Itho, T.; Mori, W.; Suzuki, S. *Inorg. Chim. Acta* **1990**, *175*, 17. (b) Yan, S.; Cheng, P.; Peng, J.; Liao, D.; Jiang, Z.; Wang, G. *Polyhedron* **1994**, *13*, 1801. (c) Zeng, W. F.; Cheng, C. P.; Wang, S. M.; Cheng, M.-C.; Lee, G.-H.; Wang, Y. *Inorg. Chem*. **1995**, *34*, 728. (d) Kayatani, T.; Hayashi, Y.; Suzuki, M.; Inomata, K.; Uehara, A. *Bull. Chem. Soc. Jpn*. **1996**, *69*, 389. (e) Cheng, P.; Liao, D.; Yan, S.; Jiang, Z.; Wang, G. *Transition Met. Chem. (London)* **1996**, *21*, 515. (f) Frey, S. T.; Murthy, N. N.; Weintraub, S. T.; Thompson, L. K.; Karlin, K. D. *Inorg. Chem*. **1997**, *36*, 956. (g) Aly, M. M. *J. Coord. Chem*. **1999**, *47*, 505. (h) Geetha, K.; Tiwary, S. K.; Chakravarty, A. R.; Ananthakrishna, G. *J. Chem. Soc., Dalton Trans.* **1999**, 4463. (i) Ku, S.-M.; Wu, C.-Y.; Lai, C. K. *J. Chem. Soc., Dalton Trans.* **2000**, 3491. (j) Gentschev, P.; Luken, M.; Moller, N.; Rompel, A.; Krebs, B. *Inorg. Chem. Commun*. **2001**, *4*, 753. (k) Averseng, F.; Lacroix, P. G.; Malfant, I.; Perisse, N.; Lepetit, C.; Nakatani, K. *Inorg. Chem*. **2001**, *40*, 3797. (l) Mikuriya, M.; Minowa, K.; Nukada, R. *Bull. Chem. Soc. Jpn*. **2002**, *75*, 2595 and references therein. (m) Cheng, P.; Zhang, L. Z.; Bu, W.-M.; Peng, J.-H.; Yan, S.-P.; Liao, D.-Z.; Jiang, Z.-H. *Z. Anorg. Allg. Chem*. **2003**, *629*, 1996. (n) Elerman, Y.; Kara, H.; Elmali, A. *Z. Naturforsch. A. Phys. Sci*. **2003**, *58*, 363 and references therein. (o) Mukherjee, A.; Saha, M. K.; Nethaji, M.; Chakravarty, A. R. *Chem. Commun*. **2004**, 716. (p) Chou, Y.-C.; Huang, S.-F.; Koner, R.; Lee, G.-H.; Wang, Y.; Mohanta, S.; Wei, H.-H. *Inorg. Chem*. **2004**, *43*, 2759 and references therein. (q) Huang, S.-F.; Chou, Y.-C.; Misra, P.; Lee, C.-J.; Mohanta, S.; Wei, H.-H. *Inorg. Chim. Acta*. **2004**, *357*, 1627. (r) Mukherjee, A.; Saha, M. K.; Nethaji, M.; Chakravarty, A. R. *Polyhedron* **2004**, *23*, 2177. (s) Mukherjee, A.; Saha, M. K.; Nethaji, M.; Chakravarty, A. R. *New J. Chem*. **2005**, *29*, 596. (t) Rossi, L. M.; Neves, A.; Bortoluzzi, A. J.; Hörner, R.; Szpoganicz, B.; Terenzi, H.; Mangrich, A. S.; Pereira-Maia, E.; Castellano, E. E.; Haase, W. *Inorg. Chim. Acta* **2005**, *358*, 1807. (u) Gupta, S.; Mukherjee, A.; Nethaji, M.; Chakravarty, A. R. *Polyhedron* **2005**, *24*, 1922. (v) Weng, C.-H.; Cheng, S.-C.; Wei, H.-M.; Wei, H.-H.; Lee, C.-J. *Inorg. Chim. Acta* **2006**, *359*, 2029.

(2) (a) Mikuriya, M.; Yamato, Y.; Tokii, T. *Inorg. Chim. Acta* **1991**, *181*, 1. (b) Mikuriya, M.; Yamato, Y.; Tokii, T. *Bull. Chem. Soc. Jpn*. **1992**, *65*, 2624. (c) Chjo, K. H.; Choi, Y. K.; Lee, S. J.; Seo, S. S. *J. Korean Chem. Soc*. **1992**, *36*, 428. (d) Pessiki, P. J.; Khangulov, S. V.; Ho, D. M.; Dismukes, G. C. *J. Am. Chem.* Soc. **1994**, *116*, 891. (e) Zhang, Z.-Y.; Brouca-Cabarrecq, C.; Hemmert, C.; Dahan, F.; Tuchagues, J.-P. *J. Chem. Soc., Dalton Trans*. **1995**, 1453 and refs. therein. (f) Mikuriya, M.; Hatano, Y.; Asato, E. *Bull. Chem. Soc. Jpn*. **1997**, *70*, 2495. (g) Palopoli, C.; Chansou, B.; Tuchagues, J.-P.; Signorella, S. *Inorg. Chem*. **2000**, *39*, 1458. (h) Palopoli, C.; González-Sierra, M.; Robles, G.; Dahan, F.; Tuchagues, J.-P.; Signorella, S. *J. Chem. Soc., Dalton Trans*. **2002**, 3813. (i) Daier, V.; Biava, H.; Palopoli, C.; Shova, S.; Tuchagues, J.-P.; Signorella, S. *J. Inorg. Biochem*. **2004**, *98*, 1806. (j) Biava, H.; Palopoli, C.; Shova, S.; De Gaudio, M.; Daier, V.; González-Sierra, M.; Tuchagues, J.-P.; Signorella, S. *J. Inorg. Biochem*. **2006**, *100*, 1660. (k) Moreno, D.; Palopoli, C.; Daier, V.; Shova, S.; Vendier, L.; González Sierra, M.; Tuchagues, J.-P.; Signorella, S. *Dalton Trans.* **2006**, 5156.

(3) (a) Fallon, G. D.; Markiewich, A.; Murray, K. S.; Quach, T. *J. Chem. Soc*. **1991**, 198. (b) Than, R.; Schrodt, A.; Westerheide, L.; Van Eldik, R.; Krebs, B. *Eur. J. Inorg. Chem*. **1999**, 1537. (c) Satcher, J. H., Jr.; Droege, M. W.; Olmstead, M. M.; Balch, A. L. *Inorg. Chem*. **2001**, *40*, 1454. (d) Westerheide, L.; Mueller, F. K.; Than, R.; Krebs, B.; Dietrich, J.; Schindler, S. *Inorg. Chem*. **2001**, *40*, 1951.

(4) (a) Volkmer, D.; Hommerich, B.; Griesar, K.; Haase, W.; Krebs, B. *Inorg. Chem*. **1996**, *35*, 3792. (b) Hommerich, B.; Schwoeppe, H.; Volkmer, D.; Krebs, B. *Z. Anorg. Allg. Chem*. **1999**, *625*, 75. (c) Elmali, A.; Kavlakoglu, E.; Elerman, Y. *Z. Naturforsch., B: Chem. Sci*. **2001**, *56*, 1315.

(5) Kayatani, T.; Hayashi, Y.; Suzuki, M.; Uehara, A. *Bull. Chem. Soc. Jpn*. **1994**, *67*, 2980.

(6) Kanamori, K.; Yamamoto, K.; Okayasu, T.; Matsui, N.; Okamoto, K.; Mori, W. *Bull. Chem. Soc. Jpn*. **1997**, *70*, 3031.

(7) Nishino, S.; Kobayashi, T.; Matsushima, H.; Tokii, T.; Nishida, Y. *Z. Naturforsch., C: J. Biosci*. **2001**, *56*, 138.

(8) Bertoncello, K.; Fallon, G. D.; Murray, K. S. *Polyhedron* **1990**, *9*, 2867 and references therein.

(9) Murase, I.; Ueno, S.; Kida, S. *Inorg. Chim. Acta* **1984**, *87*, 155.

was stirred for 30 min at room temperature. The color of the solution turned immediately to dark brown. The solution was filtered and kept in a refrigerator for crystallization. After 3 days, brown crystals of **1** formed; they were filtered out and washed with cold methanol. Yield: 0.018 g (27.8%). Upon standing in the air for a few hours, the crystals lose MeOH, pick up water, and lose crystallinity. The resulting samples analyze as $[Mn_2(L^1)(pz)(MeOH)_2(H_2O)_2]$ (Anal. Calcd for $C_{22}H_{28}Mn_2N_4O_9$: C, 43.87; H, 4.69; N, 9.30. Found: C, 43.3; H, 4.0; N, 9.5. IR (KBr pellet, cm^{-1}): 3385 (ν_{OH}), 1598 ($\nu_{C=O}$), 1237 (ν_{CO}(phenoxo)), 1043 (ν_{CO}(alkoxo)). UV−vis (λ_{max}, nm): 355, 588, 638, 666, 688.)

$[Mn_2(L^2)(pz)(MeOH)_4]$ (2). This complex was prepared as described above for **1**, using 0.034 g of H_5L^2 (0.1 mmol), 0.072 g (0.2 mmol) of $Mn(ClO_4)_2 \cdot 6H_2O$, 0.049 mL (0.5 mmol) of piperidine, and 0.014 g, (0.2 mmol) of pyrazole. After 3 days green crystals of **2** formed; they were filtered out and washed with cold methanol. Yield: 0.048 g (74.4%). Upon standing in the air for a few hours, the crystals lose MeOH, pick up water, and lose crystallinity. The resulting samples analyze as $[Mn_2(L^2)(pz)(H_2O)_4]$ (Anal. Calcd for $C_{21}H_{26}Mn_2N_4O_9$: C, 42.87; H, 4.45; N, 9.52. Found: C, 43.0; H, 3.9; N, 9.4. IR (KBr pellet, cm^{-1}): 3383 (ν_{OH}), 1598 ($\nu_{C=O}$), 1259, 1243 (ν_{CO}(phenoxo)), 1051 (ν_{CO}(alkoxo)). UV−vis (λ, nm): 348, 588, 696.)

$[Mn_2(L^1)(OAc)(MeOH)_4]$ (3). $Mn(OAc)_3 \cdot 2H_2O$ was prepared as reported.[10] To a stirred solution of $Mn(OAc)_3 \cdot 2H_2O$ (0.054 g, 0.2 mmol) in MeOH (10 mL) was added a solution of ligand (0.033 g, 0.1mmol) in 30 mL of MeOH and piperidine (0.049 mL, 0.5 mmol). The reaction mixture was stirred for 15 min at room temperature. The color of the solution turned immediately to dark greenish-brown. The solution was filtered and left to stand undisturbed for crystallization. After 3 days crystals of **3** formed; they were filtered out and washed with cold methanol. Yield: 0.02 g (32.1%). Upon standing in the air for a few hours, the crystals lose MeOH, pick up water, and lose crystallinity. The resulting samples analyze as $[Mn_2(L^1)(OAc)(MeOH)_2(H_2O)_2]$ (Anal. Calcd for $C_{21}H_{28}Mn_2N_2O_{11}$: C, 42.44; H, 4.75; N, 4.71. Found: C, 42.4; H, 4.4; N, 4.6. IR (KBr pellet, cm^{-1}): 3373 (ν_{OH}), 1602 ($\nu_{C=O}$), 1575 (ν_{COO}(asym)), 1452 (ν_{COO}(sym)), 1248 (ν_{CO}(phenoxo)), 1039 (ν_{CO}(alkoxo)). UV−vis (λ_{max}, nm): 351, 488, 532, 588, 630, 658.)

Physical Measurements. Microanalyses for C, H, and N were performed by the Microanalytical Laboratory of the Laboratoire de Chimie de Coordination at Toulouse, France. Infrared spectra (4000−400 cm^{-1}) were recorded on a Perkin-Elmer Spectrum GX system 2000 FT-IR spectrometer as KBr pellets. The electronic spectra (diffuse reflectance technique) were recorded with a UV4 UNICAM spectrophotometer in the range 280−820 nm with MgO as reference. 1D ^1H NMR spectra were acquired at 250.13 MHz on a Bruker WM250 spectrometer. 1D ^{13}C spectra using ^1H broad-band decoupling $\{^1H\}^{13}C$ and ^1H decoupling with selective proton irradiation were obtained with a Bruker WM250 facility working at 62.89 MHz. Chemical shifts are given in ppm versus TMS (^1H and ^{13}C) using $(CD_3)_2SO$ as solvent. Variable-temperature (1.8−300 K) magnetic susceptibility data were collected on freshly prepared crystalline samples of the complexes with a Quantum Design MPMS SQUID susceptometer under a 0.1 T applied magnetic field. Data were corrected with the standard procedure for the contribution of the sample holder and for diamagnetism of the sample.[11]

Crystallographic Data Collection and Structure Determination for 1−3. Crystals of **1**−**3** were kept in the mother liquor until they were covered with oil, attached to glass fibers, and quickly cooled to 180 K. The selected crystals of **1** (brown, 0.37 × 0.18 × 0.15 mm^3) and **2** (green, 0.1 × 0.12 × 0.35 mm^3) were mounted on an Oxford-Diffraction XCALIBUR CCD diffractometer using a graphite-monochromated Mo Kα radiation source (λ = 0.710 73 Å) and equipped with an Oxford Cryosystems Cryostream cooler device. The selected crystal of **3** (dark brown-greenish, 0.2 × 0.2 × 0.1 mm^3) was mounted on a Stoe Imaging Plate Diffractometer System (IPDS) using a graphite monochromator (λ = 0.710 73 Å) and equipped with an Oxford Cryosystems cooler device. The data were collected at 180 K. The unit cell determination and data integration were carried out using the CrysAlis package[12] for **1** and **2** and Xred[13] for **3**. A total of 26 815 reflections were collected for **1**, of which 15 203 were independent (R_{int} = 0.0341), 12 707 reflections for **2**, of which 6965 were independent (R_{int} = 0.0259), and 13 027 reflections for **3**, of which 4837 were independent (R_{int} = 0.1375).

The structure of **1** was solved by direct methods using SHELXS-97.[14] The structures of **2** and **3** were solved using SIR 92.[15] Refinements were carried out by full-matrix least squares on F^2 with SHELXL-97[16] included in the software package WinGX.[17] For complex **3**, the O*H* hydrogen atoms of the methanol molecules were first derived from Fourier difference maps, but as the refinement was unstable, they were finally fixed. The remaining hydrogen atoms were included in calculated positions and refined as riding atoms using SHELX default parameters. All non-hydrogen atoms were refined with anisotropic displacement parameters. Absorption corrections were applied using Multiscan[18] (**1** and **2**) or DELABS[19] (**3**). The figures were drawn with Cameron.[20] Crystal data collection and refinement parameters are collated in Table 1.

Results and Discussion

Synthesis. The ligands were synthesized by condensation of phenyl salicylate with the corresponding 1,*n*-diamino-*n′*-hydroxyalkanes (*n*, *n′* = 3, 2 and 4, 2) in the presence of triethylamine, in propan-2-ol. The reactions were carried out in the presence of NEt_3 to avoid possible protonation of the primary amine functions before their reaction to form the amide bonds and also to avoid monocondensation of the diamine with formation of "half-unit" ligands.[21] The synthesis of complexes **1** and **2** was accomplished by reaction of diluted methanolic solutions of $Mn(ClO_4)_2 \cdot 6H_2O$, H_5L^1 (**1**) or H_5L^2 (**2**), and pyrazole, in the presence of piperidine. Formation of these complexes involves aerial oxidation of Mn^{II} to Mn^{III} and full deprotonation of H_5L^1 and H_5L^2 to $[L^1]^{5-}$ and $[L^2]^{5-}$, respectively. Complexes **1** and **2** are the first ever described doubly bridged μ-alkoxo-μ-pyrazolato dinuclear Mn^{III} complexes of pentaanionic pentadentate

(10) Brauer, G., Ed. *Handbook of Preparative Inorganic Chemistry*; Academic Press: New York, 1965; Vol. 2, pp 1469−1470.
(11) Pascal, P. *Ann. Chim. Phys*. **1910**, *19*, 5.
(12) *CrysAlis RED*, version 1.170.32; Oxford Diffraction Ltd.: Oxford, U.K., 2003.
(13) *STOE: IPDS Manual*, version 2.75; Stoe & Cie: Darmstadt, Germany, 1996.
(14) Sheldrick, G. M. *SHELXS-97: Program for the Solution of Crystal Structures*; University of Göttingen: Göttingen, Germany, 1997.
(15) Altomare, A.; Cascarano, G.; Giacovazzo, C.; Guagliardi, A.; Burla, M. C.; Polidori, G.; Camalli, M. *J. Appl. Crystallogr*. **1994**, *27*, 435.
(16) Sheldrick, G. M. *SHELXL-97, Program for the Refinement of Crystal Structures*; University of Göttingen: Göttingen, Germany, 1997.
(17) Farrugia, L. J. *J. Appl. Crystallogr*. **1999**, *32*, 837.
(18) Blessing, R. H. *Acta Crystallogr., Sect. A* **1995**, *51*, 33.
(19) Walker, N.; Stuart, D. DELABS. *Acta Crystallogr*. **1983**, *A39*, 158.
(20) Watkin, D. J.; Prout, C. K.; Pearce, L. J. *CAMERON*; Chemical Crystallography Laboratory, University of Oxford: Oxford, U.K., 1996.

Table 1. X-ray Crystallographic Data for the Mn^{III} Complexes $[Mn_2(L^1)(pz)(MeOH)_4]\cdot 0.5MeOH$ (**1**), $[Mn_2(L^2)(pz)(MeOH)_4]$ (**2**), and $[Mn_2(L^1)(OAc)(MeOH)_4]$ (**3**)

param	**1**	**2**	**3**
chem formula	$C_{24.5}H_{34}Mn_2N_4O_{9.5}$	$C_{25}H_{34}Mn_2N_4O_9$	$C_{23}H_{32}Mn_2N_2O_{11}$
fw	646.215	644.44	622.39
space group	$P\bar{1}$	$P\bar{1}$	$P\bar{1}$
a, Å	12.2050(7)	9.4560(5)	10.511(5)
b, Å	12.7360(8)	11.0112(5)	11.713(5)
c, Å	19.2780(10)	13.8831(6)	13.135(5)
α, deg	99.735(5)	90.821(4)	64.401(5)
β, deg	96.003(4)	92.597(4)	74.000(5)
γ, deg	101.221(5)	93.403(4)	66.774(5)
V, Å^3	2867.6(3)	1441.29(12)	1329.3(10)
Z	4	2	2
T, K	180	180	180
λ, Å	0.710 73	0.710 73	0.710 73
ρ_{calcd}, g·cm^{-1}	1.497	1.485	1.555
μ(Mo Kα), mm^{-1}	0.939	0.932	1.011
R^a [$I > 2\sigma(I)$]	0.0519	0.0426	0.0911
wR^b [$I > 2\sigma(I)$]	0.1284	0.1030	0.2237
R^a (all data)	0.0841	0.0624	0.1685
wR^b (all data)	0.1459	0.1101	0.2648

^{a} $R = \Sigma||F_o| - |F_c|/\Sigma|F_o|$. ^{b} $wR = [\Sigma w(|F_o^2| - |F_c^2|)^2/\Sigma w|F_o^2|^2]^{1/2}$.

ligands including amido donors. Complex **3** was synthesized by reaction of diluted methanolic solutions of $Mn(OAc)_3\cdot 2H_2O$ and H_5L^1 in the presence of piperidine. Attempts to obtain the μ-alkoxo-μ-acetato dinuclear complex incorporating $[L^2]^{5-}$ were unsuccessful. Complexes **1**−**3** are not soluble in common solvents, which precluded carrying out solution studies to gain some insight into their reactivity and electrochemical properties.

Description of the Structures. Structure of $[Mn_2(L^1)(pz)(MeOH)_4]\cdot 0.5MeOH$ (1). The crystals of **1** contain two crystallographically independent molecules having similar structural features. An ORTEP view of one molecule is shown in Figure 1. Selected bond distances and angles are collated in Table 2. The molecular structure of the dinuclear complex **1** shows that the two manganese ions are bridged by an alkoxo oxygen of the pentaanionic ligand and a pyrazolato anion. The ligand is almost planar. The carbon atom bound to O13 (alkoxo oxygen atom) is disordered over two locations, C19A (62%) and C19B (38%). The coordination polyhedra of the Mn^{III} centers may be described as elongated octahedra. The equatorial plane of each Mn is formed by phenoxo-oxygen, amido-nitrogen, and alkoxo-oxygen donor atoms of $[L^1]^{5-}$ and by a pyrazolato nitrogen atom (1.834−2.034 Å range), while the axial positions are occupied by the oxygen atom of methanol molecules with significantly longer bond distances (2.249−2.436 Å range). These bond distances are comparable to those reported for other dinuclear manganese(III) complexes.[2a,b,g,k]

The intramolecular metal−metal separations (Mn1···Mn2 and Mn11···Mn12) and the angles Mn2−O3−Mn1 and Mn11−O13−Mn12 defining the core of the two crystallographically independent molecules are virtually identical, 3.3956(6) and 3.3965(7) Å and 126.33(9) and 126.69(10)°, respectively. The intramolecular Mn···Mn distance is longer than those observed in triply bridged bis(*μ*-alkoxo)-*μ*-acetato dinuclear manganese(III) complexes[2b,g,k] and shorter than that in the doubly bridged *μ*-alkoxo-*μ*-acetato dinuclear manganese(III) complex.[8] The $Mn-O_{alkoxo}-Mn$ angle is larger than those of triply bridged bis(*μ*-alkoxo)-*μ*-acetato dinuclear manganese(III) complexes[2b,g,k] and smaller than that of the doubly bridged *μ*-alkoxo-*μ*-acetato dinuclear manganese(III) complex.[8]

The crystal packing of **1** consists in 1D infinite chains developing alternately along two directions (Figure 2). This 1D supramolecular network results from hydrogen-bonding interactions between the axially coordinated methanol molecules and the amido-oxygen atoms from adjacent dinuclear molecules of **1**. The methanol lattice molecule is also involved in a strong $O_{methanol}-H\cdots O_{amido}$ hydrogen bond (D−H···A, *d* (Å), ∠ (deg): O6−H56···O8, 2.74, 154; O7−H57···O2$^{\#2}$, 2.77, 176; O8−H58···O4$^{\#1}$, 2.56, 168; O9−H59···O2$^{\#2}$, 2.69, 171; O16−H160···O14$^{\#4}$, 3.15, 167; O17−H170···O12$^{\#3}$, 2.66, 167; O18−H180···O14$^{\#4}$, 2.57, 179; O19−H190···O100$^{\#3}$, 2.73, 160; O100−H100···O12, 2.74, 165; symmetries (#1) $-x, -y, -z + 1$, (#2) $-x, -y + 1, -z + 1$, (#3) $-x + 1, -y + 1, -z$, (#4) $-x + 1, -y + 2, -z$).

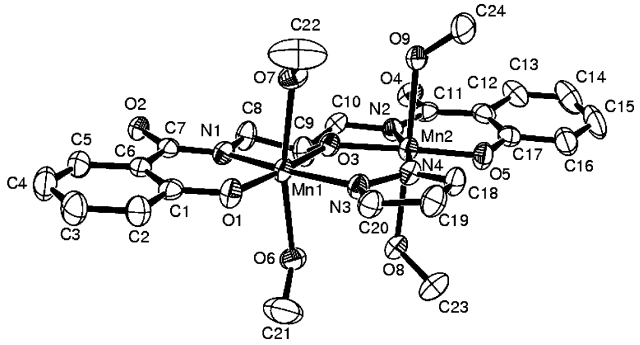

Figure 1. Plot of one of the two independent molecules of $[Mn_2(L^1)(pz)(MeOH)_4]\cdot 0.5MeOH$ (**1**) at the 30% probability level with atom numbering. Hydrogen atoms are omitted for clarity.

(21) (a) Patra, A. K.; Ray, M.; Mukherjee, R. *Inorg. Chem.* **2000**, *39*, 652. (b) Kido, T.; Nagasato, S.; Sunatsuki, Y.; Matsumoto, N. *Chem. Commun.* **2000**, 2113. (c) Costes, J.-P.; Dahan, F. *C. R. Acad. Sci. Paris Chim.* **2001**, *4*, 97. (d) Rowland, J. M.; Thornto, M. L.; Olmstead, M. M.; Mascharak, P. K. *Inorg. Chem.* **2001**, *40*, 1069. (e) Jiménez, C. A.; Belmar, J. B. *Tetrahedron* **2005**, *61*, 3933.

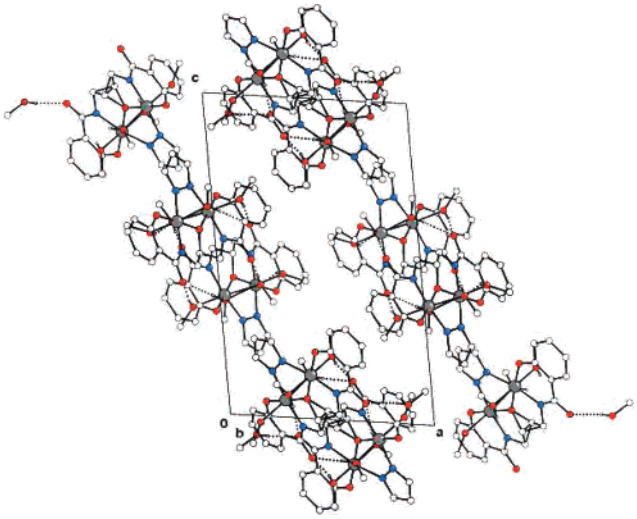

Figure 2. View of the crystal packing of **1** in a plane perpendicular to *b*, showing 1D chains of hydrogen-bonded molecules. Hydrogen atoms not involved in H-bonds are omitted for clarity.

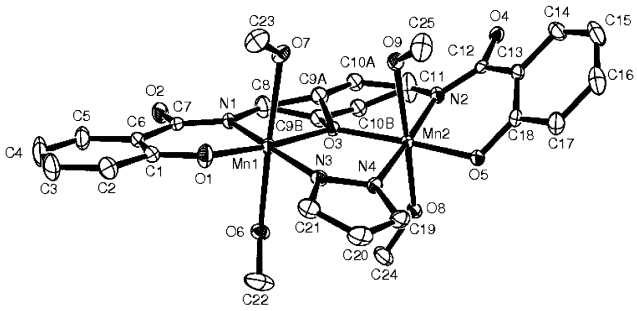

Figure 3. Plot of $[Mn_2(L^2)(pz)(MeOH)_4]$ (**2**) at the 30% probability level with atom numbering showing the relative conformations of the A and B stereoisomers. Hydrogen atoms are omitted for clarity.

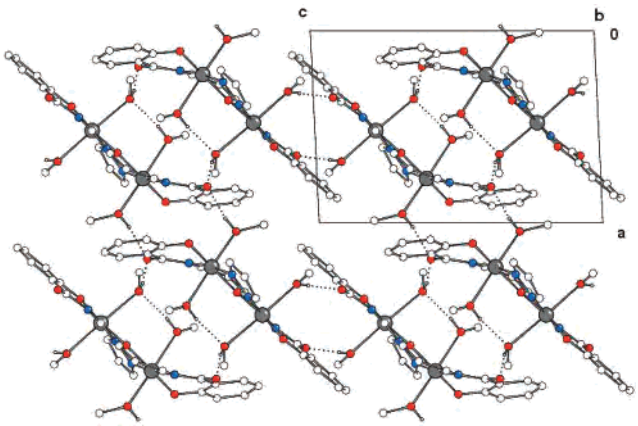

Figure 4. Crystal packing diagram of $[Mn_2(L^2)(pz)(MeOH)_4]$ (**2**): View perpendicular to the *b*-axis showing the hydrogen bonds which develop along the *a* and *c* directions. For clarity, only one stereoisomer is shown and hydrogen atoms not involved in H-bonds are omitted.

Structure of $[Mn_2(L^2)(pz)(MeOH)_4]$ (2). At variance with **1**, the crystals of **2** contain only one crystallographically independent dinuclear molecule having structural features similar to those of both independent molecules in **1**. An ORTEP view of the molecule is shown in Figure 3, while the relevant bond distances and angles are listed in Table 3. Atoms C9 and C10 are statistically disordered over locations A and B with an occupancy factor of 0.5. H_5L^2 is dissymmetrical and includes an asymmetric carbon atom, C9: in this study, we used the racemic mixture of H_5L^2 and the two resulting stereoisomers (Figure 3) are present in the unit cell of the achiral crystal of complex **2** ($P\bar{1}$ space group).

Similarly to **1**, the coordination polyhedra of the Mn^{III} centers may be described as elongated octahedra. The equatorial plane of each Mn is formed by phenoxo-oxygen, amido-nitrogen, and alkoxo-oxygen donor atoms of $[L^2]^{5-}$ and by a pyrazolato nitrogen atom (1.839−2.028 Å range), while the axial positions are occupied by the oxygen atom of methanol molecules with significantly longer bond distances (2.190−2.417 Å range). The $Mn-O_{alkoxo}$ bond distances are slightly longer than in complex **1**. The bonding geometry around the alkoxo oxygen atom O3 is planar, the sum of the three bond angles around O3 being ≈359°. However, the coordination mode of $[L^2]^{5-}$ is not planar, the angle between the phenyl rings being 52° vs 7 and 12° for the two independent molecules in **1**. It is also worth noting that while the equatorial coordination planes and the pyrazolato mean-plane are roughly coplanar in **1** (7 and 3°), they significantly depart from coplanarity in **2** (13°). The distance Mn1···Mn2 (3.4282(5) Å) is similar, but the Mn1−O3−Mn2 angle (123.15(8)°) is smaller than that in complex **1** (126.33(9)° and 126.69(10)°).

The crystal packing of **2** consists in 2D sheets (Figure 4) which result from hydrogen-bonding interactions similar to those found in complex **1**. The distances between hydrogen-bonded oxygen atoms are O6···O2 = 2.630(3), O8···O4 = 2.664(2), O7···O4 = 2.616(2), and O9···O7 = 2.741(2) Å.

Structure of $[Mn_2(L^1)(OAc)(MeOH)_4]$ (3). A complex similar to **3** has been described in the literature:[8] $[Mn_2(L^1)(OAc)(py)_4]\cdot py\cdot H_2O$ (**3′**). The molecular structure of **3** is shown in Figure 5, and selected bond distances and angles are listed in Table 4. The two manganese ions are bridged by the alkoxo oxygen atom of the fully deprotonated ligand and the acetato anion.

The bonding geometry around the alkoxo oxygen atom O3 is almost planar, the sum of the three bond angles around O3 (≈356°) being very close to those in **1** (≈355°) and **2** (≈359°). The $Mn-O_{alkoxo}$ distances in the acetato-bridged complexes **3** and **3′** are nearly equal to each other, 1.938−1.955 Å range, but longer than those in the pyrazolato-bridged complex **1** (1.894−1.907 Å range). In spite of this small difference, the coordination polyhedra of the Mn^{III} centers in **3** may be described, similarly to **1** and **2**, as elongated octahedra. The equatorial plane of each Mn is formed by phenoxo-oxygen, amido-nitrogen, and alkoxo-oxygen donor atoms of $[L^1]^{5-}$ and by an acetato oxygen atom (1.837−1.985 Å range), and the axial positions are occupied by the oxygen atom of methanol molecules with significantly longer bond distances (2.246−2.405 Å range). The apical donor atoms in complex **3**, which are roughly perpendicular to the NO_3 equatorial planes, deviate by more than 10° from linearity: O9−Mn1−O8 = 169.5(2)° and O10−Mn2−O11 = 168.5(3)°, while the corresponding angles range from 168.36(8) to 176.53(8)° in the pyrazolato-bridged complex **1**. The Mn1···Mn2 distance in **3** (3.541(3) Å) is similar to

Table 2. Selected Bond Distances (Å) and Angles (deg) for $[Mn_2(L^1)(pz)(MeOH)_4]\cdot 0.5MeOH$ (**1**)

Mn1−N1	1.948(2)	Mn1−N3	2.034(2)	Mn1−O1	1.8381(19)	Mn1−O3	1.9045(18)
Mn1−O6	2.277(2)	Mn1−O7	2.279(2)	Mn2−N2	1.928(2)	Mn2−N4	2.020(2)
Mn2−O3	1.9009(18)	Mn2−O5	1.8347(19)	Mn2−O8	2.436(2)	Mn2−O9	2.249(2)
Mn11−N11	1.948(2)	Mn11−N13	2.026(2)	Mn11−O11	1.836(2)	Mn11−O13	1.894(2)
Mn11−O16	2.299(2)	Mn11−O17	2.249(2)	Mn12−N12	1.938(2)	Mn12−O15	1.8344(19)
Mn12−O13	1.9065(19)	Mn12−N14	2.020(2)	Mn12−O18	2.326(2)	Mn12−O19	2.309(2)
N1−Mn1−O6	91.39(9)	N1−Mn1−O7	96.26(8)	N3−Mn1−O6	86.41(8)	N3−Mn1−O7	84.51(8)
O1−Mn1−N1	93.19(9)	O1−Mn1−N3	97.01(9)	O1−Mn1−O6	94.31(8)	O1−Mn1−O7	94.02(8)
O3−Mn1−N1	83.25(8)	O3−Mn1−N3	86.59(8)	O3−Mn1−O6	87.28(8)	O3−Mn1−O7	84.93(8)
N2−Mn2−O8	93.82(8)	N2−Mn2−O9	91.38(9)	N4−Mn2−O8	84.13(8)	N4−Mn2−O9	90.22(9)
O3−Mn2−N2	83.03(9)	O3−Mn2−N4	86.45(8)	O3−Mn2−O8	86.99(7)	O3−Mn2−O9	90.75(8)
O5−Mn2−N2	94.29(9)	O5−Mn2−N4	96.14(9)	O5−Mn2−O8	90.22(8)	O5−Mn2−O9	92.30(9)
N11−Mn11−O16	93.42(10)	N11−Mn11−O17	88.31(9)	N13−Mn11−O16	87.91(10)	N13−Mn11−O17	89.76(9)
O11−Mn11−N11	94.87(10)	O11−Mn11−N13	95.20(9)	O11−Mn11−O16	91.33(9)	O11−Mn11−O17	92.08(9)
O13−Mn11−N11	83.48(9)	O13−Mn11−N13	86.49(9)	O13−Mn11−O16	87.34(9)	O13−Mn11−O17	89.30(8)
N12−Mn12−O18	91.91(10)	N12−Mn12−O19	90.60(9)	N14−Mn12−O18	86.50(9)	N14−Mn12−O19	91.44(8)
O13−Mn12−N12	83.46(9)	O13−Mn12−N14	86.45(9)	O13−Mn12−O18	90.60(9)	O13−Mn12−O19	92.05(8)
O15−Mn12−N12	94.40(9)	O15−Mn12−N14	95.64(9)	O15−Mn12−O18	87.77(9)	O15−Mn12−O19	89.67(8)

Table 3. Selected Bond Distances (Å) and Angles (deg) for $[Mn_2(L^2)(pz)(MeOH)_4]$ (**2**)

Mn1−N1	1.915(2)	Mn1−N3	2.006(2)	Mn2−N2	1.968(2)	Mn2−N4	2.028(2)
Mn1−O1	1.8390(17)	Mn1−O3	1.9472(15)	Mn2−O3	1.9511(15)	Mn2−O5	1.8530(16)
Mn1−O6	2.2719(18)	Mn1−O7	2.4171(18)	Mn2−O8	2.1895(17)	Mn2−O9	2.3339(17)
N1−Mn1−O3	86.31(7)	N1−Mn1−O6	88.61(8)	N2−Mn2−O8	90.66(8)	N2−Mn2−O9	87.13(7)
N1−Mn1−O7	95.30(7)	N3−Mn1−O6	88.08(7)	N4−Mn2−O8	96.19(7)	N4−Mn2−O9	86.08(7)
N3−Mn1−O7	88.03(7)	O1−Mn1−N1	94.06(8)	O3−Mn2−N2	94.45(7)	O3−Mn2−N4	86.06(7)
O1−Mn1−N3	91.98(8)	O1−Mn1−O6	91.05(8)	O3−Mn2−O8	92.82(7)	O3−Mn2−O9	84.33(6)
O1−Mn1−O7	88.71(8)	O3−Mn1−N3	88.04(7)	O5−Mn2−N2	91.01(8)	O5−Mn2−N4	88.36(8)
O3−Mn1−O6	95.34(7)	O3−Mn1−O7	84.90(6)	O5−Mn2−O8	88.53(7)	O5−Mn2−O9	94.54(7)
Mn1−O3−C9A	112.2(3)	Mn1−O3−C9B	111.7(3)	Mn2−O3−C9A	123.5(3)	Mn2−O3−C9B	123.5(3)

that found in **3′** (3.552(2) Å) but is longer than that of the pyrazolato-bridged complex **1**, as a consequence of the longer three-atom bridge in **3** and **3′**. The Mn1−O3−Mn2 angle in **3**, 130.9(3)°, is slightly smaller than the corresponding angle reported for **3′**, 132.5(2)°, but larger than those found in complex **1** (126.33(9) and 126.69(10)°).

The crystal packing of **3** consists in 1D infinite zigzag chains (Figure 6) resulting from intermolecular hydrogen-bonding interactions involving the axially coordinated methanol molecules and the amido-oxygen atoms. All apically coordinated methanol molecules participate in intramolecular hydrogen bonds. The diffraction data are not good enough to allow determining the location of the O*H* hydrogen atoms of the methanol molecules (*d*, Å: O8···O2 = 2.593(8), O9···O4 = 2.801(10), O10···O4 = 2.697(9), O11···O8 = 2.811(9)).

UV−Vis Spectroscopy. The dinuclear Mn^{III} complexes **1**−**3** exhibit solid-state electronic spectra typical of a high-spin d^4 electron configuration.[2b] The spectra are characterized by several absorption bands in the region ranging from 348 to 696 nm. The strong absorption around 350 nm (also present in the spectra of H_5L^1 and H_5L^2) is ligand related. Probably due to the very broad solid state absorptions, LMCT bands from phenoxo oxygens are not clearly visible. The weaker low-energy absorptions (488−696 nm) are assigned to d−d transitions. These spectral features are consistent with the elongated octahedral environment of manganese(III) ions.[2b,22]

Magnetic Properties. The magnetic susceptibility of complexes **1**−**3** has been measured in the 1.8−300 K

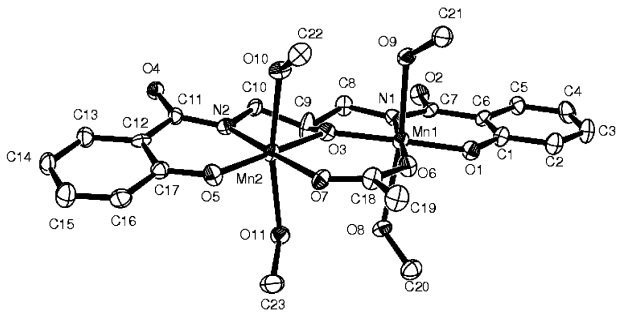

Figure 5. Plot of $[Mn_2(L^1)(OAc)(MeOH)_4]$ (**3**) at the 30% probability level with atom numbering. Hydrogen atoms are omitted for clarity.

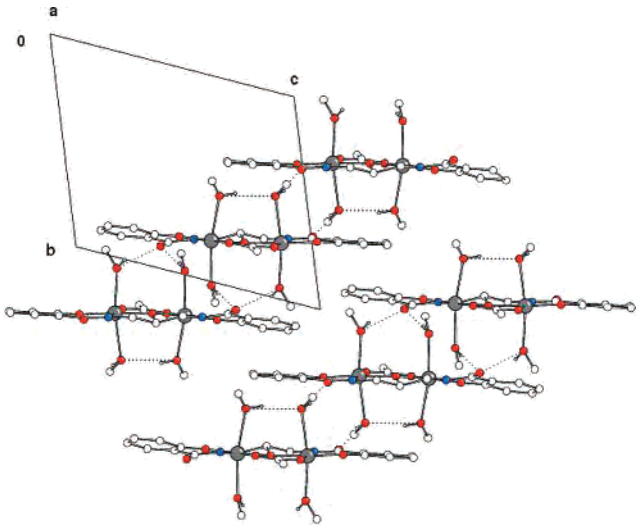

Figure 6. Crystal packing diagram of $[Mn_2(L^1)(OAc)(MeOH)_4]$ (**3**) showing 1D zigzag chains formed by hydrogen bonds in a plane perpendicular to *a*. Hydrogen atoms not involved in H-bonds are omitted for clarity.

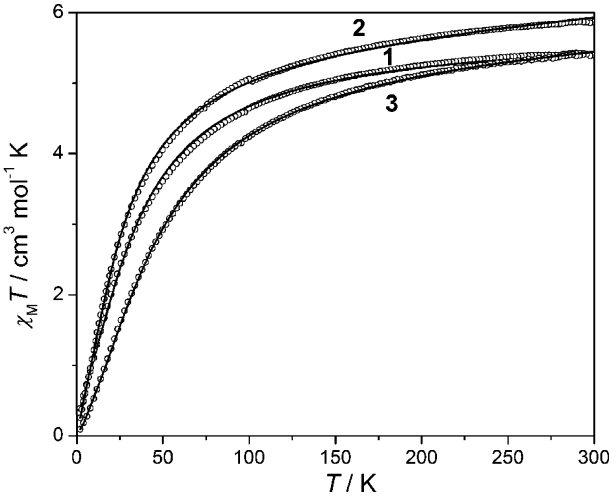

Figure 7. $\chi_M T$ vs T data for $[Mn_2(L^1)(pz)(MeOH)_4]\cdot 0.5MeOH$ (**1**), $[Mn_2(L^2)(pz)(MeOH)_4]$ (**2**), and $[Mn_2(L^1)(OAc)(MeOH)_4]$ (**3**). The circles are measured data, and the lines are the best fits based on the Hamiltonian of eq 1 (see text).

temperature range, under an applied magnetic field of 0.1 T. The $\chi_M T$ product of all three dinuclear compounds decreases upon cooling (Figure 7), suggesting operation of antiferromagnetic interactions between Mn^{III} ions.

The magnetic susceptibility, χ_M, increases from values of 0.018 (**1**, **3**) and 0.019 (**2**) cm^3 mol^{-1} at 300 K to broad maxima of 0.123 and 0.064 cm^3 mol^{-1} at ~13 and ~28 K for **2** and **3**, respectively, typical of antiferromagnetic interactions. Characteristic paramagnetic tails appear below ~5 K. The corresponding maximum of **1** is masked by the paramagnetic tail and appears as a shoulder around 15 K. The values of $\chi_M T$ are 5.4 (**1**, **3**) and 5.7 (**2**) cm^3 mol^{-1} K at 300 K, which is lower than the spin-only value for two noninteracting $S = 2$ metal centers (6.00 cm^3 mol^{-1} K). These values and the presence of maxima in the χ_M vs T data are both indications of antiferromagnetic interactions. The same conclusion may be drawn from the constant drop of $\chi_M T$ upon decreasing temperature. The slight increase of χ_M below 7 K is attributed to the presence of a small fraction of paramagnetic impurity (p%). To fit these experimental data, a simple system of two exchange-coupled manganese(III) ions was considered.[23] Initial attempts to fit the data with this simple model yielded satisfactory results only for **1**, with discrepancies at lower temperatures for **2** and **3**. Considering the lattice structures of the complexes, we may assume the interplay of H-bond-mediated intermolecular magnetic interactions. On the other hand, the axially elongated octahedral coordination spheres of the Mn^{III} led us to assume that zero-field splitting effects might be operative. Introduction of an intermolecular interaction according to the mean-field $\hat{H} = -2zJ\langle S_z\rangle\hat{S}_z$ Hamiltonian afforded a slight improvement to the fits of **2** and **3**, while the improvement to the fit of **1** was marginal. Introducing, however, a zero-field splitting term D, common for both manganese sites ($D_1 = D_2 = D$), brought about significant improvements to the fits of **2** and **3**. On the other hand, the improvement to the fit of **1** was also marginal. It was thus decided that this was the most appropriate model for the interpretation of our data. The implemented Hamiltonian was[24]

$$\hat{H} = -2J\hat{S}_{Mn1}\hat{S}_{Mn2} + D(\hat{S}_{zMn1}{}^2 + \hat{S}_{zMn2}{}^2) \qquad (1)$$

This model reproduced the experimental curve very well, except for small disagreements at low temperature, which may be due to simultaneous operation of intermolecular interactions between adjacent dinuclear molecules through the weak $O_{amido}\cdots O_{methanol}$ contacts yielding 1D chains (**1**, **3**) or 2D sheets (**2**) (see Description of Structures). However, since intermolecular interactions brought marginal improvements to the fits of **2** and **3**, and to avoid overparametrization, only zero-field splittings were considered. The parameter values for the best fits, shown as solid lines in Figure 7, were as the following: $J = -3.6(3)$ cm^{-1}, $D \approx 0$ cm^{-1}, $g = 1.93(6)$, $p = 3.3\%$ (**1**); $J = -2.7(3)$ cm^{-1}, $D = 0.8(2)$ cm^{-1}, $g = 1.93(6)$, $p = 1.5\%$ (**2**); $J = -4.9(4)$ cm^{-1}, $D = 3.8(3)$ cm^{-1}, $g = 1.95(5)$, $p = 0.5\%$ (**3**).

The J, D, g, and structural parameter values significant for magneto−structural correlations (Mn···Mn distance and Mn−O_{alkoxo}−Mn angle) of compounds **1**−**3** are collated in Table 5, together with those of other μ-alkoxo-bridged dinuclear manganese(III) complexes including one auxiliary bridge.

Compounds **1**−**3** including one alkoxo bridge associated with one pyrazolato (acetato) bridge are characterized by large Mn···Mn distances (3.40−3.54 Å) and Mn−O_{alkoxo}−Mn angles in the 123−131° range. The −2.7 to −4.9 cm^{-1} range of J values for this first series is not very broad in agreement with the small Δ(Mn···Mn) and Δ(Mn−O_{alkoxo}−Mn) ranges. The small absolute values of J agree with overlap through the 2p oxygen orbitals, and the small prevalence of antiferromagnetic vs ferromagnetic interactions is in keeping with the quite large values of the Mn−O_{alkoxo}−Mn angle.

The compounds in lines 4−6 including one alkoxo bridge associated with one N−C−C−O bridge from the second pentadentate ligand are characterized by slightly larger Mn···Mn distances (3.76−3.82 Å) and Mn−O_{alkoxo}−Mn angles in the 125−129° range. Similarly to the previous series, the −3.6 to −5.8 cm^{-1} range of J values for this second series is not very broad in agreement with the small Δ(Mn···Mn) and Δ(Mn−O_{alkoxo}−Mn) ranges. Again, the small absolute values of J agree with overlap through the 2p oxygen orbitals and the small prevalence of antiferromagnetic vs ferromagnetic interactions is in keeping with the quite large values of the Mn−O_{alkoxo}−Mn angle (125−129°). However, due to (i) the four-atom auxiliary bridge vs the two- or three-atom auxiliary bridge in **1**−**3**, (ii) the slightly larger Mn···Mn distances, and (iii) the overlapping ranges of Mn−O_{alkoxo}−Mn angles, we would not expect slightly larger J values than for **1**−**3**. On the other hand, we note that the J

(22) (a) Dingle, R. *Acta Chem. Scand.* **1966**, *20*, 33. (b) Boucher, L. J.; Day, V. W. *Inorg. Chem.* **1977**, *16*, 1360. (c) Arulsamy, N.; Glerup, J.; Hazell, A.; Hodgson, D. J.; McKenzie, C. J.; Toftlund, H. *Inorg. Chem.* **1994**, *33*, 3023.

(23) O'Connor, C. J. *Prog. Inorg. Chem.* **1982**, *29*, 203.

(24) Garge, P.; Chikate, R.; Padhye, S.; Savariault, J. M.; De Loth, P.; Tuchagues, J.-P. *Inorg. Chem.* **1990**, *29*, 3315 and references therein.

Table 4. Selected Bond Distances (Å) and Angles (deg) for $[Mn_2(L^1)(OAc)(MeOH)_4]$ (**3**)

Mn1−N1	1.962(7)	Mn1−O1	1.837(7)	Mn2−N2	1.958(8)	Mn2−O3	1.955(6)
Mn1−O3	1.939(7)	Mn1−O6	1.985(6)	Mn2−O5	1.837(7)	Mn2−O7	1.985(6)
Mn1−O8	2.405(7)	Mn1−O9	2.261(7)	Mn2−O10	2.246(7)	Mn2−O11	2.291(7)
N1−Mn1−O8	93.2(3)	N1−Mn1−O9	92.6(3)	N2−Mn2−O10	93.6(3)	N2−Mn2−O11	95.7(3)
O1−Mn1−N1	93.5(3)	O1−Mn1−O6	87.2(3)	O3−Mn2−N2	83.9(3)	O3−Mn2−O7	95.4(3)
O1−Mn1−O8	92.9(3)	O1−Mn1−O9	95.4(3)	O3−Mn2−O10	87.7(3)	O3−Mn2−O11	86.5(2)
O3−Mn1−N1	83.1(3)	O3−Mn1−O6	96.3(2)	O5−Mn2−N2	91.7(3)	O5−Mn2−O7	89.1(3)
O3−Mn1−O8	84.9(3)	O3−Mn1−O9	87.2(3)	O5−Mn2−O10	95.7(3)	O5−Mn2−O11	90.8(3)
O6−Mn1−O8	86.3(2)	O6−Mn1−O9	87.8(3)	O7−Mn2−O10	85.5(3)	O7−Mn2−O11	85.2(3)

Table 5. Magnetic Parameters for Complexes **1**−**3** and Related Dinuclear Mn^{III} Complexes

complex	J (cm^{-1})	D (cm^{-1})	g	Mn···Mn (Å)	Mn−O−Mn (deg)	ref
1	−3.6	0	1.93	3.396	126.5	
2	−2.7	0.8	1.93	3.428	123.2	
3	−4.9	3.8	1.95	3.541	130.9	
$[Mn^{III}_2(5Cl\text{-}salpro)_2(MeOH)]$[a]	−3.6		1.95	3.808	128.9	25
$[Mn^{III}_2(salpro)_2(thf)]$[b]	−5.5		2.00	3.756	124.5	26
$[Mn^{III}_2(salpro)_2(H_2O)]$[b]	−5.8		2.00	3.818	126.0	27
$[Mn^{III}(3NO_2\text{-}salpro)]_2\cdot 2dmf$[c]	−1.6	−2.5	2.06	3.223	100.5	2e
$[Mn^{III}L]_2\cdot 2MeCN$[d]	+4.5		2.00	3.243	100.7	28
$[Mn^{III}_2L'(OMe)Cl_2(MeOH)_2]$[e]	−15.6		2.01	3.006	101.6	2b
$[Mn^{III}_2L'(OMe)(NCO)_2(H_2O)_2]$[e]	−16.5		2.00	2.980	100.3	2b

[a] 5Cl-salpro = 1,3-bis(5-chlorosalicylidenamino)propan-2-ol. [b] salpro = 1,3-bis(salicylidenamino)propan-2-ol. [c] $3NO_2$-salpro = 1,3-bis(3-nitrosalicylidenamino)propan-2-ol. [d] L = 1-salicylamino-3-salicylidenaminopropan-2-ol. [e] L′ = 1,5-bis(salicylidenamino)pentan-3-ol.

ranges overlap (−3.6 to −5.8 cm^{-1} vs −2.7 to −4.9 cm^{-1}) and the difference between these two ranges may be not significant because the two series of compounds do not pertain to the same structural type and also while the interpretation of the experimental data take both J and D for the first series, it only takes J into account for the second one.

Concerning **1**−**3**, the $Mn-O_{alkoxo}-Mn$ bridging angle seems to be the essential factor determining the magnitude of the antiferromagnetic exchange interaction. As previously discussed, this angle decreases in the order **3** (130.9°) > **1** (126.5°(average)) > **2** (123.2°), and the J value (Table 5) decreases in the same order. More precisely, the J magnitude shows a linear correlation ($J = -3.49\theta + 113.83$, $R = 0.99975$) with the Mn−O−Mn angle θ for complexes **1**−**3**, which exhibit similar coordination spheres and bridging modes.

Although the common characteristic of compounds in lines 7−10 is that, in addition to the alkoxo bridge common to all compounds of Table 5, they include one additional alkoxo bridge, thus imposing virtually the same $Mn-O_{alkoxo}-Mn$ angle of ∼100°, they exhibit significant differences. The compounds in lines 7 and 8 include alkoxo bridges from two identical pentadentate ligands and are characterized by still large Mn···Mn distances (3.22−3.24 Å range): the small $Mn-O_{alkoxo}-Mn$ angles (∼100°) then diminishes the already small prevalence of antiferromagnetic vs ferromagnetic interactions (line 7, −1.6 cm^{-1}) or allows a small prevalence of ferromagnetic vs antiferromagnetic interactions (line 8, +4.5 cm^{-1}). Moreover, three significant differences between the compounds in lines 7 and 8 may be at the origin of their marked difference in magnetic behavior (antiferromagnetic vs ferromagnetic). In the case of $[Mn^{III}(3NO_2\text{-}salpro)]_2\cdot 2dmf$[2e] (line 7), (i) each pentadentate ligand bridges the two Mn centers through its alkoxo oxygen atom, (ii) the $3NO_2$-salpro pentadentate ligands include two imine nitrogen donors, and (iii) the experimental data concern the 2−300 K range and their interpretation takes both J and D into account. In the case of $[Mn^{III}L]_2\cdot 2MeCN$[28] (line 8), (i) each pentadentate ligand wraps around one Mn center and the alkoxo oxygen atom of each $[Mn^{III}L]$ component is also bonded to the Mn center of the second $[Mn^{III}L]$ component but with a larger Mn−O distance (2.27 vs 1.94 Å) yielding dissymmetrical bridges, (ii) the dissymmetrical L (1-salicylamino-3-salicylidenaminopropan-2-ol) pentadentate ligands include one amine and one imine nitrogen donors yielding a less delocalized and less rigid coordination environment to the Mn centers, and (iii) the experimental data concern the 80−300 K range and their interpretation takes only J into account. While part iii may affect only the absolute value of J, parts i and ii imply quite different structural and electronic characteristics which affect the nature of the interaction.

Finally, the additional alkoxo bridge for the compounds in lines 9 and 10 originates from a methoxo anion, conferring an overall geometry similar to that in compounds **1**−**3** (first series of Table 5). Together with the larger N···O^-···N bite of L′, these two monatomic bridges impose a shorter Mn···Mn distance (∼3 Å) that allows not only larger overlap through the 2p oxygen orbitals but also possibly weak through-space overlap of the $3d_{xy}$ orbitals leading to larger antiferromagnetic contributions to the bulk magnetic interaction.

(25) Bonadies, J. A.; Kirk, M. L.; Lah, M. S.; Kessissoglou, D. P.; Hatfield, W. E.; Pecoraro, V. L. *Inorg. Chem.* **1989**, *28*, 2037.
(26) Bertoncello, K.; Fallon, G. D.; Murray, K. S.; Tiekink, E. R. T. *Inorg. Chem.* **1991**, *30*, 3562.
(27) Mikuriya, M.; Yamato, Y.; Tokii, T. *Bull. Chem. Soc. Jpn.* **1992**, *65*, 1466.
(28) Mikuriya, M.; Yamato, Y.; Tokii, T. *Chem. Lett.* **1992**, 1571.

The obtained *D* values are in the range of those previously reported.[2e,29] Positive *D* parameters are usually associated with either tetragonal compression or trigonal bipyramidal five-coordination.[29a,30] However, by considering the interaction between the ground state and LMCT states with the valence bond configuration interaction (VBCI) model, it has been recently shown that *D* can be positive for tetragonally elongated Mn^{III} complexes.[31] Nevertheless, we recall that the sign of *D* cannot be safely determined from magnetic susceptibility data alone; therefore, sign attribution is only tentative.

Conclusions

In this paper we report on the first examples of doubly bridged μ-alkoxo-μ-pyrazolato dinuclear manganese(III) complexes. The X-ray diffraction analysis revealed that complexes **1**−**3** consist of dinuclear units which are further extended into 1D (**1** and **3**) or 2D (**2**) supramolecular networks via hydrogen-bonding interactions involving the noncoordinated amido-oxygen atoms of the pentadentate ligands and coordinated methanol-oxygen atoms. These interactions are likely to play an important role in the stabilization of the crystal molecular structures. The magnetic behavior of these doubly bridged μ-alkoxo-μ-pyrazolato (or acetato) species is dominated by intradinuclear antiferromagnetic superexchange interactions suggesting that the intermolecular interactions operating through the extended network of $OH_{methanol}\cdots O_{amido}$ contacts are too weak to play a significant role in the magnetic properties of these manganese(III) complexes.

Acknowledgment. Financial support by the Agence Universitaire de la Francophonie (AUF), through a postdoctoral grant "Bourse de Perfectionnement en Recherche" to L.S., and by the European Community, through a postdoctoral grant to A.T.-V. within the framework of the TMR Contract FMRX-CT980174, is gratefully acknowledged.

Supporting Information Available: X-ray crystallographic files in CIF format for compounds **1**−**3**. This material is available free of charge via the Internet at http://pubs.acs.org.

IC062398R

(29) (a) Kennedy, B. J.; Murray, K. S. *Inorg. Chem.* **1985**, *24*, 1557. (b) Wieghardt, K. *Angew. Chem., Int. Ed.* **1989**, *28*, 1153. (c) Thorp, H. H.; Brudvig, G. W. *New J. Chem.* **1991**, *15*, 479.

(30) Whittaker, J. W.; Whittaker, M. M. *J. Am. Chem. Soc.* **1991**, *113*, 5528.

(31) (a) Mossin, S.; Weihe, H.; Barra, A. L. *J. Am. Chem. Soc.* **2002**, *124*, 8764. (b) Costes, J.-P.; Dahan, F.; Donnadieu, B.; Rodriguez Douton, M.-J.; Bousseksou, A.; Tuchagues, J.-P. *Inorg. Chem.* **2004**, *43*, 2736.